

Journal Pre-proofs

Synergistic catalytic effect between ultrasound waves and pyrimidine-2,4-diamine-functionalized magnetic nanoparticles: Applied for synthesis of 1,4-dihydropyridine pharmaceutical derivatives

Reza Taheri-Ledari, Jamal Rahimi, Ali Maleki

PII: S1350-4177(19)31019-3

DOI: <https://doi.org/10.1016/j.ultsonch.2019.104737>

Reference: ULTSON 104737

To appear in: *Ultrasonics Sonochemistry*

Received Date: 30 June 2019

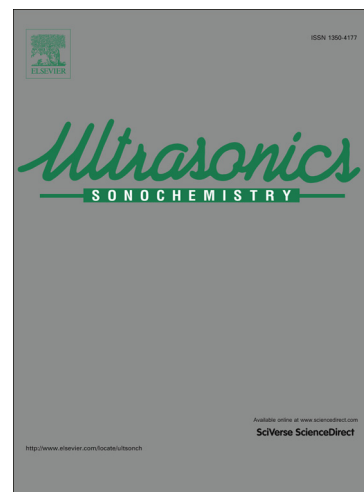
Revised Date: 10 August 2019

Accepted Date: 18 August 2019

Please cite this article as: R. Taheri-Ledari, J. Rahimi, A. Maleki, Synergistic catalytic effect between ultrasound waves and pyrimidine-2,4-diamine-functionalized magnetic nanoparticles: Applied for synthesis of 1,4-dihydropyridine pharmaceutical derivatives, *Ultrasonics Sonochemistry* (2019), doi: <https://doi.org/10.1016/j.ultsonch.2019.104737>

This is a PDF file of an article that has undergone enhancements after acceptance, such as the addition of a cover page and metadata, and formatting for readability, but it is not yet the definitive version of record. This version will undergo additional copyediting, typesetting and review before it is published in its final form, but we are providing this version to give early visibility of the article. Please note that, during the production process, errors may be discovered which could affect the content, and all legal disclaimers that apply to the journal pertain.

© 2019 Published by Elsevier B.V.



functionalized magnetic nanoparticles: Applied for synthesis of 1,4-dihydropyridine pharmaceutical derivatives

Reza Taheri-Ledari, Jamal Rahimi, Ali Maleki*

Catalysts and Organic Synthesis Research Laboratory, Department of Chemistry, Iran University of Science and Technology, Tehran 16846-13114, Iran

**Corresponding author. Tel.: +98 21 73228313; fax: +98 21 73021584. E-mail address: maleki@iust.ac.ir (A. Maleki).*

Abstract

A convenient strategy for synthesis of the various derivatives of 1,4-dihydropyridine (1,4-DHP), as one of the most important pharmaceutical compounds, is presented in this study. For this purpose, firstly, magnetic iron oxide nanoparticles (Fe_3O_4 NPs) were fabricated and suitably coated by silica network (SiO_2) and trimethoxy vinylsilane (TMVS). Then, their surfaces were well functionalized with pyrimidine-2,4-diamine (PDA) as the main active sites for catalyzing the synthesis reactions. In this regard, the performance of three different methods including reflux, microwave (MW) and ultrasound wave (USW) irradiations have been comparatively monitored via studying various analyses on the fabricated nanocatalyst ($\text{Fe}_3\text{O}_4/\text{SiO}_2$ -PDA). Concisely, high efficiency of the USW irradiation (in an ultrasound cleaning bath with a frequency of 50 kHz and power of 250 W/L) has been well proven through the investigation of the main factors such as excellent surface-functionalization, core/shell structure conservation, particle uniformity, close size distribution of the particles, and great inhibition of the particle aggregation. Then, the effectiveness of the USW irradiation as a promising co-catalyst agent has been clearly demonstrated in the 1,4-DHP synthesis reactions. It has been concluded that the USW could provide more appropriate conditions for activation of the catalytic sites of $\text{Fe}_3\text{O}_4/\text{SiO}_2$ -PDA NPs. However, high reaction yields (89%) have been obtained in the short reaction times (10 min) due to the substantial synergistic effect between the presented nanocatalyst and USW.

Keywords: *Sonochemistry; Multicomponent reaction; Iron oxide nanoparticles; Dihydropyridine; Heterogeneous catalyst*

1. Introduction

Dihydropyridine (DHP) derivatives are one of the most important categories of the pharmaceutical compounds that are extremely used as a well-known calcium channel blockers for treatment of hypertension [1,2]. The useful DHP derivatives such as amlodipine, aranidipine, barnidipine and etc. are typically prepared through multicomponent synthetic reactions. For instance, p-toluenesulfonic acid monohydrate as a Brønsted- acid has been used to catalyze the multicomponent synthetic reaction of DHP derivatives, by Xie *et al.* [3]. Furthermore, Jiang *et al.* have employed porcine pancreatic lipase as an efficient catalyst for DHP preparation [4]. Also, in our research group, DHP derivatives have been synthesized through using a guanidine-functionalized magnetic nanocatalyst [5]. Among various methods and strategies, ultrasound waves (USW) irradiation has been reported as an effective driving force supporter for DHP derivatives preparation with high performance. Reportedly, a catalyst-free synthesis protocol for functionalized DHP derivatives involving four components under USW irradiation has been introduced, by Shabalala *et al.* [6]. Additionally, a CuI-catalyzed multicomponent synthetic reaction for DHP preparation under USW irradiation, has been reported by Tabassum *et al.* [7].

In recent decade, the synergistic effects between USW with different frequencies, and nanomaterials have been extremely investigated, as well [8–10]. It seems that the co-efficiency of nanoscale catalysts with USW irradiation provides a substantial conditions for chemical and biochemical applications. As a distinguished newly reported example, the synergistic efficacy of low-frequency and low-intensity USWs combined with amphotericin B-loaded poly(lactic-co-glycolic acid) nanoparticles (as an antifungal agent) against *C. albicans* biofilms, has been investigated and the results have revealed that the activity, biomass, and proteinase and phospholipase activities of biofilms are remarkably decreased after the combination treatment of nanoparticles (NPs) with 42 kHz of USW irradiation, at an intensity of 0.30 W/cm² for 15 min [11]. In addition of the synergistic effects, the agglomeration of the nanoscale particles, as an undesirable event in various fields of chemistry and biochemistry, is inhibited through applying the USW irradiation [12]. In this regard, we use this

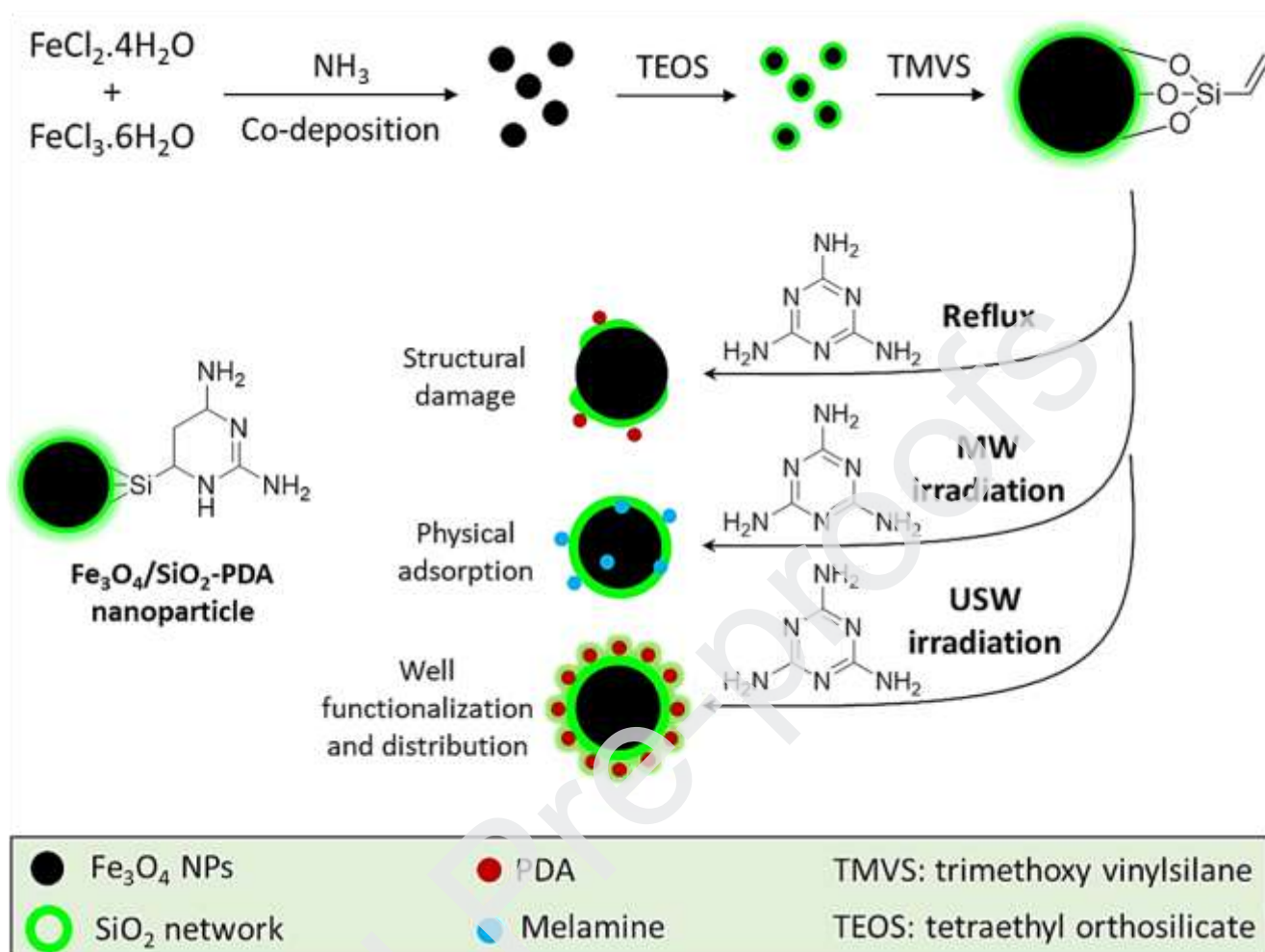
diamine (PDA)-functionalized silica-coated magnetic nanocatalyst ($\text{Fe}_3\text{O}_4/\text{SiO}_2\text{-PDA}$), made of a core/shell structure including iron oxide (Fe_3O_4) NPs as magnetic cores. Previously, we reported DHP derivatives preparation catalyzed with guanidinylated chitosan magnetic nanoscale biocomposite with acceptable yields (~89%) [5]. We have also reported some novel functionalized organic-inorganic hybrid NPs with magnetic property that were prepared via one-pot Diels-Alder approach and could be individually used as nanoscale heterogeneous organocatalysts [13]. Experiments revealed that among those novel synthesized compounds, $\text{Fe}_3\text{O}_4/\text{SiO}_2\text{-PDA}$ NPs in which melamine was loaded onto the surface of the silica-coated Fe_3O_4 NPs, show a substantial catalytic activity for DHP preparation reactions, in the presence of USWs.

Since, researchers are always following novel strategies to perform the complex synthetic reactions with more convenience, numerous tools and methods have been discovered that facilitate these synthetic processes [14]. Recently, synergistic effects between the individual facilitators has led researchers to design more intricate systems in which two or more effective factors are involved [15]. The first and foremost advantage of this strategy is accelerating the catalytic processes and obtaining higher reaction yields in the shorter reaction times, under milder conditions. As it was referred above, one of the most effective facilitators in chemical reactions is USW, which could act as a great partner for catalytic aims. Thus, in this study, we try to compare the efficacy of three different methods including reflux, microwave (MW) irradiation and USW irradiation, for preparation of $\text{Fe}_3\text{O}_4/\text{SiO}_2\text{-PDA}$ NPs via Diels-Alder approach. For this aim, vinyl-coated $\text{Fe}_3\text{O}_4/\text{SiO}_2$ NPs and melamine were used as dienophile and diene moieties of [4+2] cycloaddition reaction, respectively. Furthermore, the co-efficiency of $\text{Fe}_3\text{O}_4/\text{SiO}_2\text{-PDA}$ nanocatalyst and USW irradiation and their synergistic effect for catalyzing the DHP derivatives synthetic reactions is precisely investigated.

2.1. US-assisted preparation of Fe_3O_4/SiO_2 -PDA NPs

One of the most important points for modification of NPs is to provide suitable reaction conditions for their surfaces. It would obtain more importance if they have magnetic behavior because they are absorbed to the magnet during the magnetically stirring. In addition, particle aggregation is an inevitable event due to their magnetic property and intense preference to agglomeration. In this case, magnetic NPs could not be well dispersed and as a result their surfaces are not finely functionalized with the desired organic compounds. Therefore, we have to apply more intense conditions or extend the reaction time and use auxiliaries like metal ions to increase surface functionalization ratios, and in many cases the core/shell structure of silica coated- Fe_3O_4 NPs would collapse. In this regard, we made an effort to make a comparison between various methods applied for functionalization of the Fe_3O_4 magnetic NPs with DPA via Diels-Alder approach (Scheme 1). In our previous report, we have investigated surface functionalization of vinyl-modified silica-coated Fe_3O_4 NPs via palladium(II)-catalyzed Diels-Alder approach under reflux condition to prove that this approach is well executed onto the surface of these heterogeneous NPs [13]. In this study, firstly, we try to make a precise comparison between three different methods (reflux, MW and USW irradiations) to obtain the most suitable method for preparation of Fe_3O_4/SiO_2 -PDA magnetic NPs. Then, the synergistic catalytic effect between USWs and Fe_3O_4/SiO_2 -PDA NPs is carefully investigated for synthesis of 1,4-dihydropyridine derivatives as an important category of the pharmaceutical compounds. For this purpose, magnetic iron oxide NPs were initially synthesized through co-deposition method from iron(II) and iron(III) chloride salts in basic condition, according to the instructions explained in our previous reports [13,16,17]. Next, the core coating process by tetraethyl orthosilicate (TEOS) and trimethoxy vinylsilane (TMVS) were carried out, as presented in Scheme 1. Table 1 briefly reports various reaction times and PDA-functionalization ratios in different reaction conditions that are investigated in our assessment. From Table 1, it can be easily deduced that the most suitable condition is provided by ultrasonication (50 KHz) in water for 2 h, at 50 °C. In this regard, firstly, the

conditions, then other products were synthesized in the optimal conditions.



Scheme 1. Synthetic pathway of $\text{Fe}_3\text{O}_4/\text{SiO}_2\text{-PDA}$ nanocatalyst via reflux, MW and USW radiations, as three different methods (US bath: power density 250 W L^{-1} and frequency 50 kHz).

Table 1. Reaction condition optimization of Fe₃O₄/SiO₂-PDA nanocatalyst preparation via reflux, MW and USW radiations, as three different methods.

Entry	Method	Solvent	Condition	Time (h)	Nitrogen (W%)*
1	Reflux	Water	110 °C	12	2.84
2	Reflux	Water	110 °C	24	1.98
3	MW irradiation	DMSO	30% ^a	1	0
4	MW irradiation	DMSO	50%	2	0
5	USW irradiation	Water	PD: 250 W/L, F: 50 KHz, r.t.	2	3.28
6	USW irradiation	EtOH	PD: 250 W/L, F: 50 KHz, r.t.	4	2.9
7	USW irradiation	Water	PD: 250 W/L, F: 50 KHz, 50 °C	2	5.04
8	USW irradiation	DMSO	PD: 250 W/L, F: 50 KHz, 50 °C	2	3.22
9	USW irradiation	Water	PD: 250 W/L, F: 65 KHz, 50 °C	4	3.9

*Weight ratio of nitrogen atom after PDA-functionalization reactions obtained from energy dispersive X-ray (EDX) analysis, r.t.: room temperature; ^a 30% means the microwave oven is producing microwaves 30 percent of the time and is off the other 70 percent of the time; PD: ultrasonic power density, and F: ultrasonic frequency (ultrasound bath).

2.2. Method screening & characteristic analyses

To confirm this claim that USW irradiation is the most appropriate method for Fe₃O₄/SiO₂-PDA nanocatalyst preparation, several various analyses were investigated and the obtained results were precisely interpreted. Accordingly, the physical damages to the core/shell structure of NPs, low loading ratio of PDA onto the NPs surfaces, particle agglomeration and physical adsorption of the melamine onto the surface of NPs, are introduced as the main disadvantages of reflux and MW irradiation methods. In contrast, well dispersion of NPs (no particle accumulation), high uniformity,

binding onto the surface of vinyl-modified NPs (no physical adsorption of melamine), and excellent conservation from the core/shell structure were proven by these analyses. Short reaction time under mild conditions is most likely the main reason for excellent preservation from the structure in USW irradiation method. However, along high efficiency of this method for preparation of the $\text{Fe}_3\text{O}_4/\text{SiO}_2$ -PDA nanocatalyst, a significant synergistic effect between US waves and $\text{Fe}_3\text{O}_4/\text{SiO}_2$ -PDA nanocatalyst in catalyzed-synthesis reaction of 1,4-dihydropyridines is comprehensively discussed after the characterization section.

2.2.1. Fourier-transform infrared spectroscopy

According to the Fourier-transform infrared (FT-IR) spectra (Fig. 1), the main peaks related to the silica network including Si–OH, SiO–H, Si–O–Si were disappeared after PDA-functionalization reaction under reflux conditions (for 24 h). Whereas, they are observed in two other spectra at 797, 938 and 1082 cm^{-1} , respectively [16,18]. It means that under intense condition of reflux method the core/shell structure of vinyl-modified $\text{Fe}_3\text{O}_4/\text{SiO}_2$ NPs is extremely damaged and the appeared weak peaks at ca. 1635 and 3000 cm^{-1} coming from the partial loading of PDA onto the surface of NPs. In the case of MW irradiation method, all the essential peaks related to vinyl-modified $\text{Fe}_3\text{O}_4/\text{SiO}_2$ NPs such as stretching vibrations of Fe–O bond at 571 cm^{-1} , Si–OH, SiO–H, Si–O–Si (explained above), and also C=C bond at 1636 cm^{-1} are observed, but, no significant peak related to the loaded-PDA is observed in the spectrum. It seems that all of the adsorbed melamine molecules were removed from the surface through washing the NPs with ethanol and deionized water for several times. Ultimately, the clear spectrum related to $\text{Fe}_3\text{O}_4/\text{SiO}_2$ -PDA NPs that was carried out by using 65 KHz USW irradiation at 50 °C in 2 h, shows great preservation of core/shell structure and also considerable execution of covalent bindings onto the surface of NPs. The peak appeared at 1634 cm^{-1} coming from C=N bonds, and also sharp peaks at 1082, 938 and 797 cm^{-1} (assigned above), prove that PDA-functionalization reaction and the silica network preservation under USW irradiation were well performed. Additionally, as can be seen, the peak intensity of the broad peak appeared at 3346 cm^{-1}

via ultrasonication.

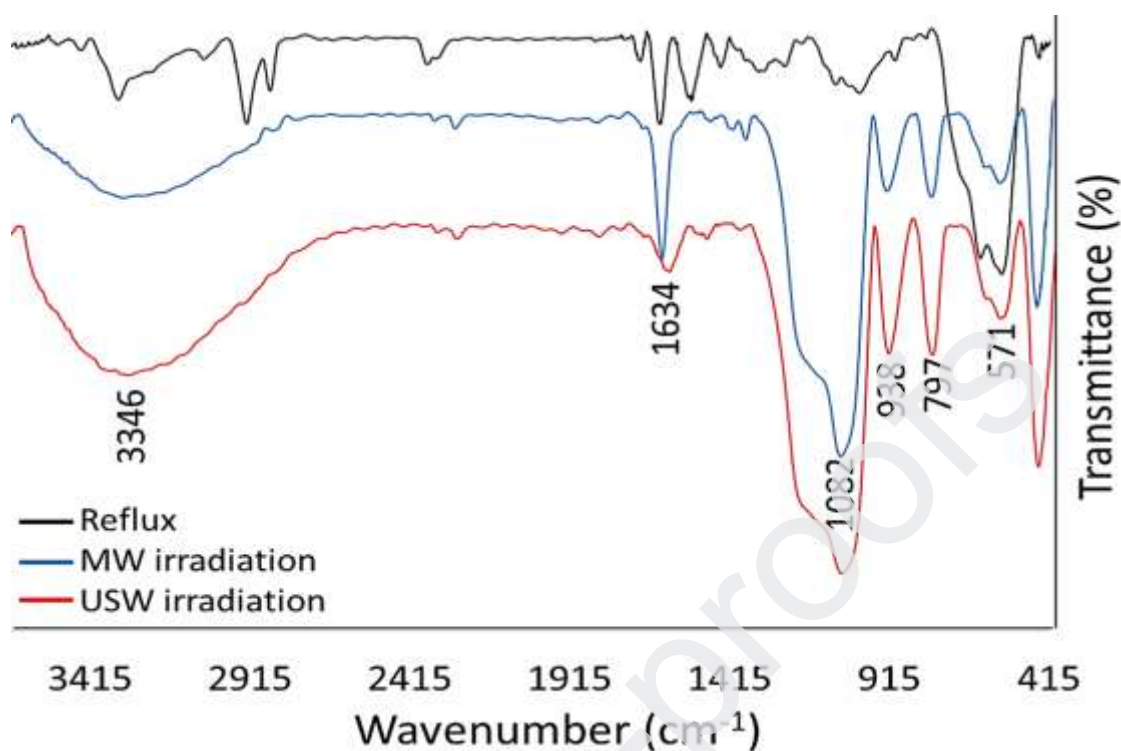


Figure 1. FT-IR spectra of desired Fe₃O₄/SiO₂-PDA NPs, obtained from three different methods reflux, MW and USW irradiations.

2.2.2. Energy-dispersive X-ray analysis

Fig. 2 shows the results of energy-dispersive spectrophotometer (EDX) analysis of produced Fe₃O₄/SiO₂-PDA NPs via three different methods. In the EDX spectra, peak intensities are corresponded to the weight ratios in the samples, as reported in the tables. As observed in the spectrum (a), the peak intensity related to silicon atom is significantly reduced. Accordingly, the related weight ratios of the loaded carbon and nitrogen atoms (belonging to PDA) onto the surface of NPs are not considerable. This observations confirm that the core/shell structure of NPs may be damaged through the reflux process. In spectrum (b), it is easily seen that the peak intensity of the silicon atom has not been declined but no nitrogen atom has been found in the sample's structure. It means that all of the melamine molecules were removed via washing the NPs and only vinyl groups were remained onto the surfaces. Therefore, this is concluded that a physical adsorption onto the surface of NPs was occurred via MW irradiation and all of the melamine molecules have been removed after washing for

intensities for silicon, carbon, and nitrogen atoms are observed in the spectrum (c), which is related to the USW's product. After well washing the NPs, observation of 5.04% of nitrogen atom in the total structure proves that covalent binding was occurred between melamine and vinyl-coated $\text{Fe}_3\text{O}_4/\text{SiO}_2$ NPs. Also, considerable peak intensity of silicon atom proves that the core/shell structure of NPs was well preserved during the ultrasonication.

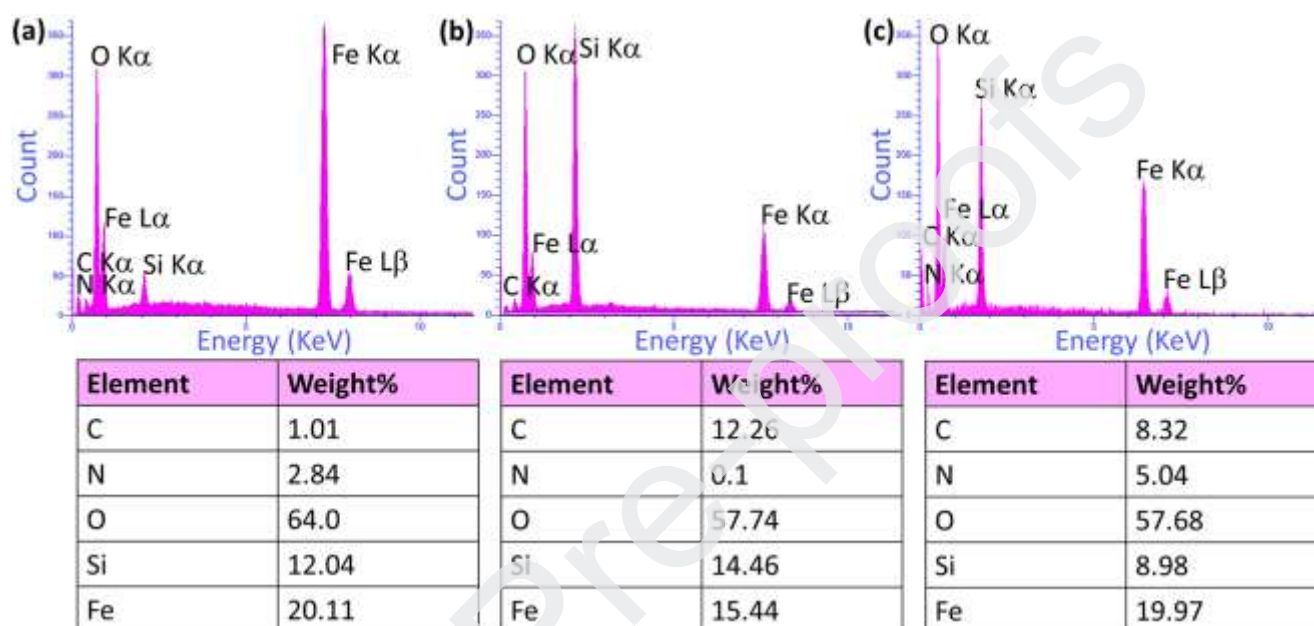


Figure 2. EDX spectra of desired $\text{Fe}_3\text{O}_4/\text{SiO}_2$ -PDA NPs and related elemental weight ratios, obtained from three different methods (a) reflux, (b) MW irradiation, and (c) USW irradiation.

2.2.3. X-ray diffraction patterns

In order to carry out more investigation on the efficiency of the applied methods, X-ray diffraction (XRD) patterns of desired products were obtained, as shown in Fig. 3. As can be seen in pattern (a) that is related to the obtained product from reflux method, the well-known broad peak (coming from the amorphous structure of silica network) at $2\theta = 25^\circ$ is almost disappeared [19]. This observation confirms that the core/shell structure has been extremely damaged under intense conditions of the reflux method. But, all of the indicator peaks of Fe_3O_4 NPs, which are marked with miller indices in the pattern, were appeared at $2\theta = 30.13, 35.23, 43.28, 57.13,$ and 62.68° . These patterns were precisely compared with the XRD pattern of Fe_3O_4 NPs according to the database of JCPDS (PDF#99-

broad peak of silica network is clearly observed, but no vestige of PDA is found in the pattern. Additionally, some of the weak peaks of Fe_3O_4 NPs like (4 0 0) were disappeared that means the surfaces of Fe_3O_4 NPs were suitably coated by TEOS and TMVS. These obtained results verify that melamine molecules were adsorbed onto the surface via MW irradiation, and they were removed through washing because they had no influence on the diffraction pattern of the prepared NPs. In contrast, as shown in pattern (c) that resulted from the USW irradiation method, a new diffraction pattern is obtained through the well execution of covalent bindings between vinyl groups and melamine structure. On the one hand, the broad peak of SiO_2 network was weakened that most likely is due to well surface coating by PDAs. Since, ultrasonication causes excellent dispersion of NPs and inhibit the particle aggregation, it is obvious that their surfaces are significantly functionalized with organic compounds. Additionally, emerging new peaks at $2\theta = 22.12, 25.8, 30.92, 40.36, 43.96, 55.56, 72.32$ and 75.84° , which have been indicated with miller indices (1 1 1), (1 0 1), (1 0 2), (1 1 2), (5 3 3) and (3 1 1), prove that a new crystal structure has been formed onto the NPs surfaces, via USW irradiation. As an additional evidence for high efficiency of the USW irradiation method, solid-state UV-vis absorbance activities of desired $\text{Fe}_3\text{O}_4/\text{SiO}_2$ -PDA NPs prepared from MW and USW irradiation methods, were compared. As expected, a partial UV-vis activity was observed for USW's product that is most likely due to the electron resonance between nitrogen atoms and a double bond in the PDA structure, while no significant UV-vis absorbance activity was observed for MW's product (Figure S21, in the SI file).

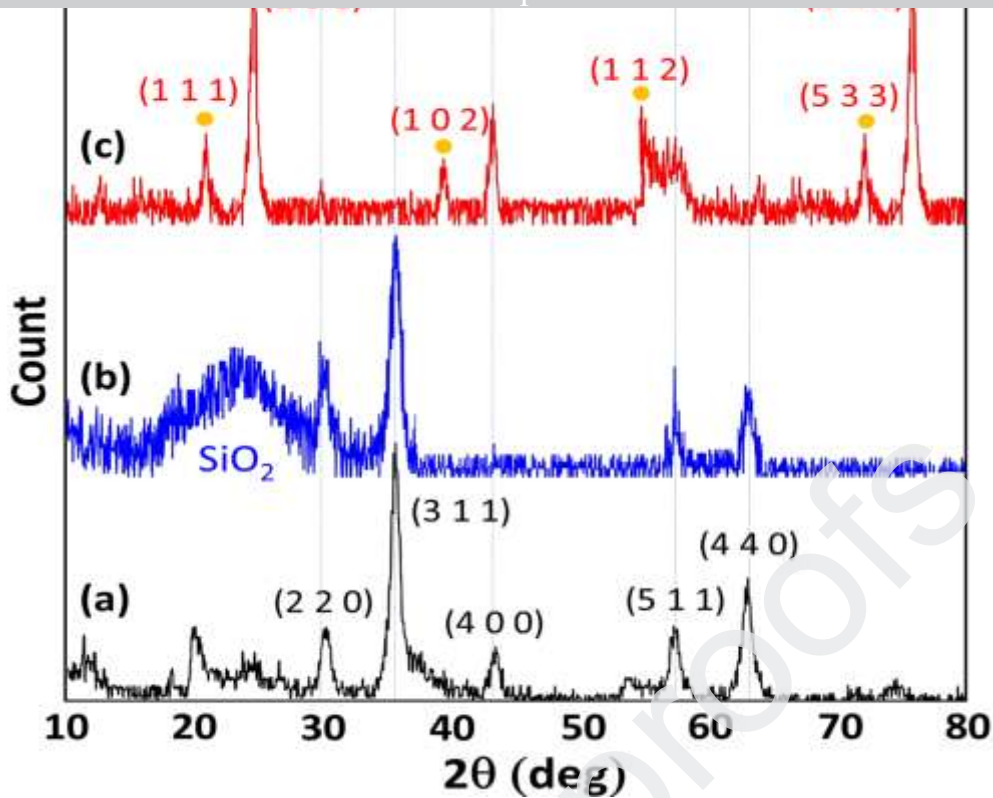


Figure 3. XRD patterns of produced $\text{Fe}_3\text{O}_4/\text{SiO}_2\text{-PDA}$ NPs via three different methods (a) reflux, (b) MW irradiation and (c) USW irradiation (●: new peak).

2.2.4. Microscopic imaging

Morphology, size, and dispersion of NPs are important factors that highlight the quality of PDA-functionalized NPs prepared by USW irradiation method. Fig. 4 illustrates the scanning electron microscopic (SEM) images of the produced $\text{Fe}_3\text{O}_4/\text{SiO}_2\text{-PDA}$ NPs via reflux (Fig. 4a), MW irradiation (Fig. 4b) and USW irradiation (Fig. 4c) methods. As shown in the images, NPs were considerably aggregated under reflux and MW irradiation conditions. This is occurred because of their superparamagnetic behavior and strong inclination to gathering, and also the lack of any proper physicommechanical force for dispersion. It seems that the particle aggregation has been more happened under MW irradiation than the reflux. This probably is because of the existence of a mechanical force (magnetic stirring) in reflux method and frequent blows to the particles by magnet. Whereas, there is no mechanical force for separation of the particles from each other in MW irradiation method. In

occurred in this method. From Fig. 4(a), this is also observed that the general morphology of the NPs has almost been deformed and gotten out from the spherical shape, under intense conditions of the reflux method. This may be because of the damage to the core/shell structure at this conditions. However, high uniformity of monodispersed NPs with well-defined spherical morphology is clearly observed in Fig. 4(c). The efficiency of these well-dispersed NPs for catalytic applications would certainly be higher than the agglomerated particles, because more active surface areas are accessible at this form. Almost, all of the produced NPs via USW irradiation have been in a range of 25–35 nm diameter, and the mean size of them was calculated in 28.5 nm for 40 particles by Digimizer software. Obviously, the main reason for this high uniformity (without any agglomeration) is the frequent physical blows by USW at a mild condition (room temperature). In addition, to obtain more confirmations for core/shell structure damaging under reflux conditions, transmission electron microscopic (TEM) imaging was also used (Figure S19, in the SI file).



Figure 4. SEM images of produced $\text{Fe}_3\text{O}_4/\text{SiO}_2\text{-PDA}$ NPs via three different methods (a) reflux, (b) MW irradiation and (c) USW irradiation.

2.2.5. Dynamic light scattering analysis

Size distribution and aggregation of the produced $\text{Fe}_3\text{O}_4/\text{SiO}_2\text{-PDA}$ NPs has also been studied by dynamic light scattering (DLS) analysis (Zetasizer), which is capable to measure bigger number of particles (in millions) in comparison with electron microscopic (EM) methods. In fact, DLS provides more robust data on size distribution and polydispersity index (PDI) in the solution phase [21]. As Fig.

two different peaks with low intensities that prove the particle agglomeration was occurred. Moreover, the large PDIs in their appeared peaks prove that there are numerous particles in various sizes (polydispersity). As can be seen in the spectra, the mean size of produced NPs via reflux and MW irradiation methods are around 42 and 60 nm, respectively. These Zeta-size values are completely corresponded with the obtained results from the SEM imaging. In contrast, a sharp slim peak with small PDI value, belonging to the USW's product (red color curve), well proves that monodispersed particles with high uniformity with a mean size of ~28 nm (confirms the SEM result), are obtained via this method. For this analysis, three different samples with 100 $\mu\text{g/mL}$ concentration were dispersed in deionized water via ultrasonication for 10 min.

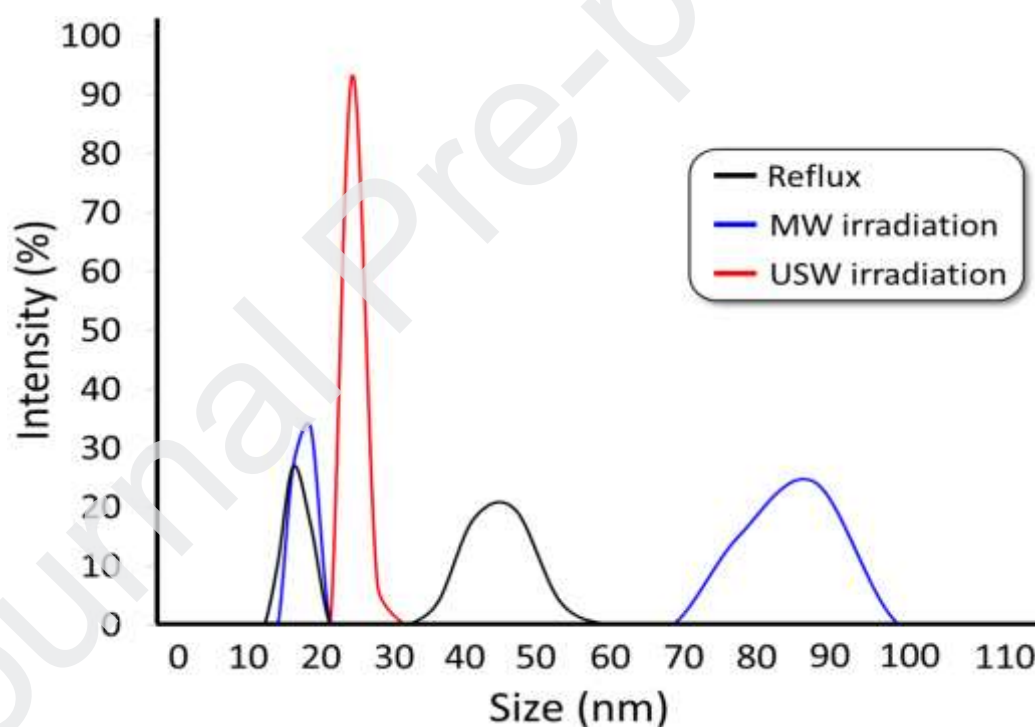


Figure 5. Intensity-based DLS data on same 100 $\mu\text{g/mL}$ dispersion of produced $\text{Fe}_3\text{O}_4/\text{SiO}_2$ -PDA NPs via three different methods.

Fig. 6a demonstrates the thermal behavior of the fabricated $\text{Fe}_3\text{O}_4/\text{SiO}_2$ -PDA NPs in a thermal range of 50-750 °C, under air atmosphere. The thermogravimetric analysis (TGA) of desired product shows that with initiating the study, a partial increase in the weight (1%) was observed. This probably is because of the physical adsorption of the moisture in the air onto the hot surfaces of NPs. Afterward, proportional to temperature rise, the weight ratio was gradually reduced to ca. 80% that is likely related to the separation of the loaded PDAs. All of the entrapped water molecules into the underlying layers like silica network, are most likely removed at this stage. Next, the second shoulder was appeared at ca. 420 °C meaning that the general structure of $\text{Fe}_3\text{O}_4/\text{SiO}_2$ NPs started to collapse. The magnetic trait of our nanoscale product was also investigated using vibrating sample magnetometer (VSM) analysis (Fig. 6b). As can be observed, the fabricated $\text{Fe}_3\text{O}_4/\text{SiO}_2$ -PDA NPs exhibit a typical super-paramagnetic behavior that facilitates the separation process of the nanocatalyst from the reaction mixture. The magnetic property of the Fe_3O_4 core is typically reduced proportional to more core coating and new layer creation onto the NPs surfaces [16,22]. Accordingly, the maximum saturation magnetization (M_s) for $\text{Fe}_3\text{O}_4/\text{SiO}_2$ -PDA NPs is occurred in 15 emu/g. It means that 40 emu/g decrease in magnetic trait is occurred through the successive core coating silica network and PDA layer [16,17].

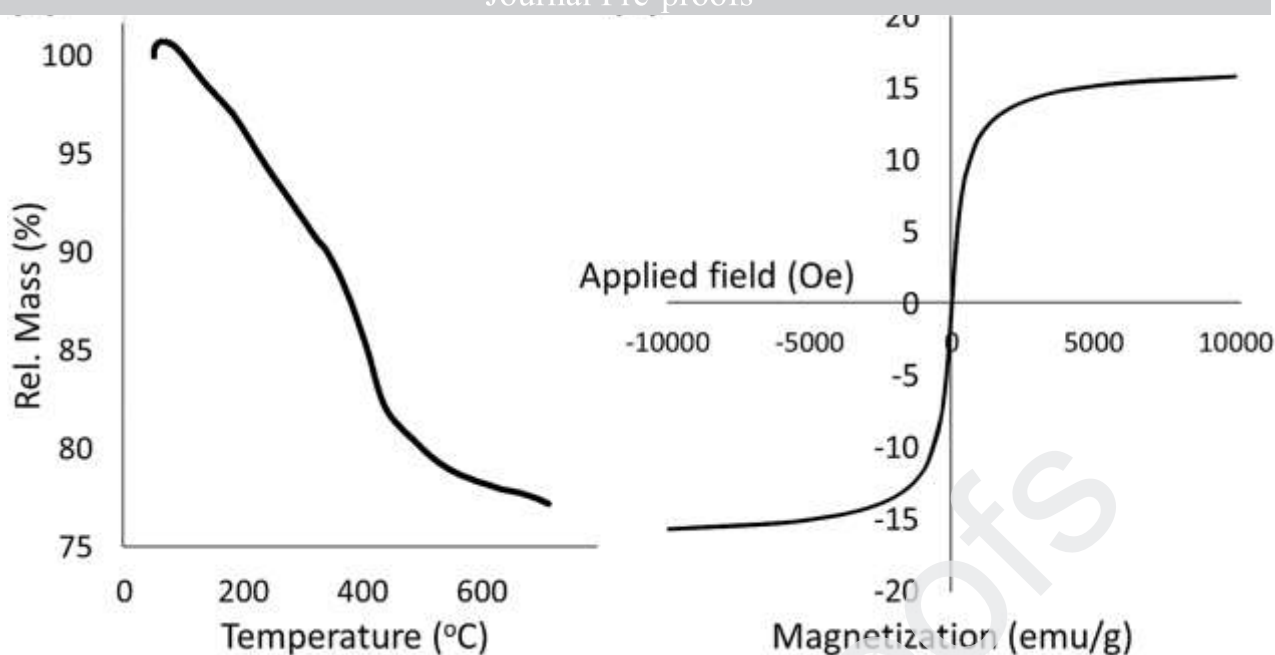


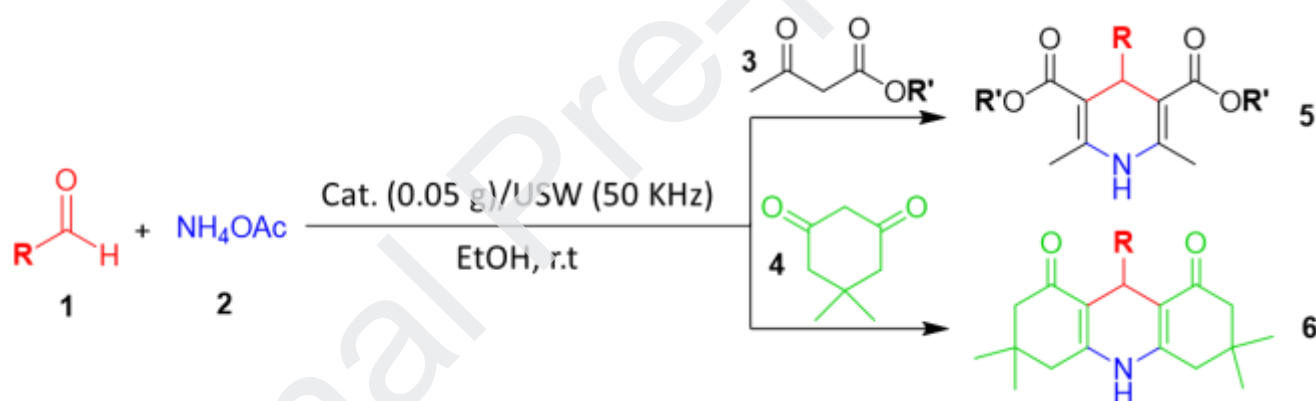
Figure 6. (a) Thermogravimetric curve, and (b) room temperature M-H curve of $\text{Fe}_3\text{O}_4/\text{SiO}_2$ -PDA NPs.

2.3. Catalytic activity of $\text{Fe}_3\text{O}_4/\text{SiO}_2$ -PDA NPs and USW

2.3.1. Synergistic catalysis effect

In order to investigate the catalytic efficiency of the produced $\text{Fe}_3\text{O}_4/\text{SiO}_2$ -PDA NPs, firstly, the reaction condition was optimized through using various solvents and catalytic ratios in the synthesis reaction of diethyl 2,6-dimethyl-4-phenyl-1,4-dihydropyridine-3,5-dicarboxylate **5a** (Scheme 2, Table 2). After using the individual $\text{Fe}_3\text{O}_4/\text{SiO}_2$ -PDA NPs and USWs as driving force supporters (Table 2, entries 1 and 2), co-efficiency of the produced nanocatalyst and USW irradiation was precisely monitored in the same synthesis reaction, and the obtained results confirmed that there is a constructive synergistic effect between $-\text{NH}_2$ groups (as active catalytic sites) and USWs. From chemical aspect, the electronic resonance in the conjugated system of the loaded PDA's structure (including nitrogen atoms and carbon-carbon double bond) is probably accelerated through frequent irradiations of the USWs and bond formation ability of the present nitrogen atoms is enhanced. In addition, the bonding energy is also provided by tiny hot bubbles that are created by USWs in an aqueous bath. From physical aspect, this is obvious that USW irradiation helps to dispersion of the

reaction. As reported in [Table 2](#), higher reaction yields were obtained through simultaneous applying both $\text{Fe}_3\text{O}_4/\text{SiO}_2$ -PDA NPs and USW irradiation, in comparison with the individual nanocatalyst. The reaction progress was monitored by thin-layer chromatography (TLC). The resulted 1,4-DHP products have also been identified by melting point measurement, FT-IR, $^1\text{H-NMR}$ and $^{13}\text{C-NMR}$ spectroscopies. According to the [Table 2](#), the highest reaction yield was obtained when 50 mg of $\text{Fe}_3\text{O}_4/\text{SiO}_2$ -PDA NPs was used in ethanol during a 10-min ultrasonication (50 KHz, at room temperature). The catalytic co-efficiency of the prepared $\text{Fe}_3\text{O}_4/\text{SiO}_2$ -PDA nanocatalyst and USW irradiation was carefully screened in the synthesis reactions of various derivatives of 1,4-DHP, as reported in [Table 3](#). The obtained results strongly support the existence of the synergistic effect between $\text{Fe}_3\text{O}_4/\text{SiO}_2$ -PDA NPs and USWs, which leads to obtain acceptable reaction yields in the short reaction times.



Scheme 2. Multicomponent synthesis route of 1,4-DHP derivatives, co-catalyzed by $\text{Fe}_3\text{O}_4/\text{SiO}_2$ -PDA NPs and USW irradiation (find R and R' in [Table 3](#)).

Table 2. Optimization of the co-catalyzed synthesis reaction of 2,6-dimethyl-4-phenyl-1,4-dihydropyridine-3,5-dicarboxylate **5a**, by Fe₃O₄/SiO₂-PDA NPs and USW irradiation.

Entry	Solvent	Cat. ^a (g)	Conditions	Time (min)	Yield ^b (%)
1	EtOH	-	Stirring at r.t.	20	Trace
2	EtOH	-	USW (50 KHz) / r.t.	20	Trace
3	EtOH	0.03	Stirring at r.t.	20	15
4	EtOH	0.04	Stirring at r.t.	20	37
5	EtOH	0.05	Stirring at r.t.	20	45
6	EtOH	0.06	Stirring at r.t.	20	47
7	EtOH	0.05	USW (50 KHz) / r.t.	20	90
8	EtOH	0.05	USW (50 KHz) / r.t.	10	89*
9	CH ₃ CN	0.05	USW (50 KHz) / r.t.	10	82
10	MeOH	0.05	USW (50 KHz) / r.t.	10	85

^a Fe₃O₄/SiO₂-PDA NPs, ^b isolated yields, * optimum conditions, r.t.: room temperature.

Table 3. The obtained yields for co-catalyzed 1,4-DHP synthesis reaction in optimum conditions (50 mg of cat., USW 50 KHz, 10 min, at room temperature).

Entry	R	R'	Product	Yield ^a (%)	MP °C		Ref.
					Found	Reported	
1	C ₆ H ₅	Et	5a	89	159-160	156-158	[23]
2	4-Cl C ₆ H ₄	Et	5b	90	147-149	144-146	[23]
3	3-NO ₂ C ₆ H ₄	Et	5c	85	162-164	162-164	[24]
4	4-NO ₂ C ₆ H ₄	Et	5d	87	129-131	130-132	[23]
5	4-Me C ₆ H ₄	Et	5e	82	133-136	133-136	[25]
6	4-OMe C ₆ H ₄	Et	5f	84	163-165	163-165	[25]
7	4-Br C ₆ H ₄	Et	5g	91	160-162	160-162	[25]
8	4-F C ₆ H ₄	Et	5h	90	153-156	153-156	[26]
9	4-OH C ₆ H ₄	Et	5i	85	227-230	227-230	[25]
10	3-OH C ₆ H ₄	Et	5j	80	187-189	187-189	[25]
11	4-CN C ₆ H ₄	Et	5k	91	194-196	194-196	[27]
12	2-Furanyl	Et	5l	80	161-163	161-163	[28]
13	Cinnamaldehyde	Et	5m	86	148-150	148-150	[25]
14	2-Thienyl	Et	5n	78	168-170	168-170	[29]
15	H ₂ CO	Et	5o	68	165-168	165-168	[25]
16	C ₆ H ₅	Me	5p	87	196-198	197-198	[30]
17	4-Cl C ₆ H ₄	Me	5q	87	196-198	195-196	[30]
18	3-NO ₂ C ₆ H ₄	Me	5r	85	209-210	210-211	[31]
19	C ₆ H ₅	-	6a	89	288-290	287	[32]
20	3-NO ₂ C ₆ H ₄	-	6b	88	295-296	293-295	[33]
21	4-NO ₂ C ₆ H ₄	-	6c	89	291-293	290-292	[33]
22	4-Cl C ₆ H ₄	-	6d	88	297-299	300	[32]
23	4-MeO C ₆ H ₄	-	6e	89	278-280	280	[32]

^a Isolated yields.

To monitor the recyclability of the produced $\text{Fe}_3\text{O}_4/\text{SiO}_2\text{-PDA}$ NPs, the NPs were magnetically collected from the reaction mixture using an external magnet after completion of the synthesis reaction. Then, the particles were well washed with ethanol and deionized water for several times, dried and used again in further reaction. Afterward, they were well dispersed in deionized water via ultrasonication, and washed again with ethanol. Finally, they were dried at $60\text{ }^\circ\text{C}$. The FT-IR spectrum, EDX spectrum and SEM image of the recycled $\text{Fe}_3\text{O}_4/\text{SiO}_2\text{-PDA}$ nanocatalyst were prepared after seven times running the process, but no significant changes in the structure were seen (Figure S22, in the SI file). It seems that the PDA-functionalized core/shell structure has an acceptable stability even after several time usages. However, reduction in the reaction yields was observed after seven times recycling and reusing in the synthesis reaction of **5a**, that probably coming from the chemical poison, loss of the some catalyst NPs during the separations, agglomeration, and etc. (Fig. 7).

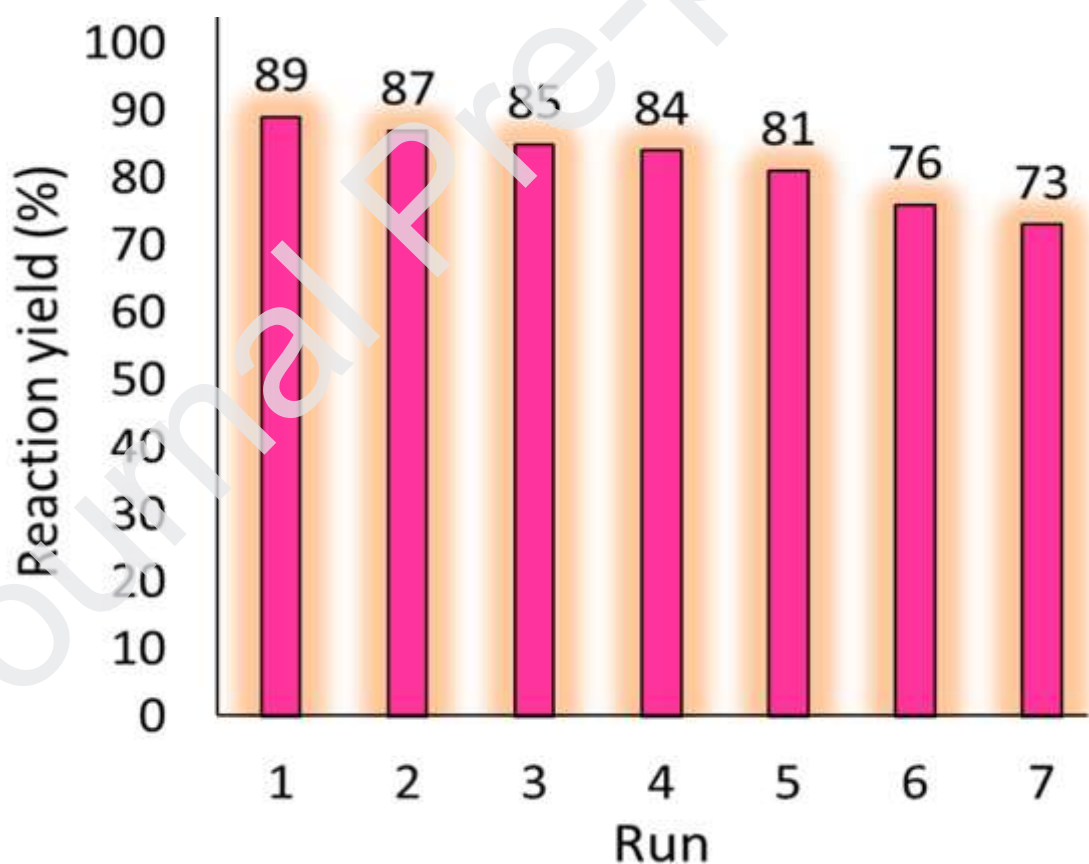


Figure 7. The catalysis reusability investigation in the synthesis reactions of **5a**, catalyzed by $\text{Fe}_3\text{O}_4/\text{SiO}_2\text{-PDA}$ NPs in the presence of USW.

3.1. Materials and equipment

All solvents, chemicals, and reagents were purchased from Merck. FT-IR spectra were obtained by Shimadzu FT-IR-8400s. EDX spectra were recorded on VEGA-TESCAN-XMU. SEM images were prepared with MIRA3TESCAN-XMU. XRD measurements were carried out by using a DRON-8 X-ray diffractometer. Melting points were measured on an Electrothermal 9100 apparatus. Thermal analysis (TGA) was done by using of Bahr-STA 504 instrument under argon atmosphere. The magnetic properties of sample were detected at room temperature using a VSM (Meghnatis Kavir Kashan Co., Kashan, Iran). NMR spectra were prepared with Varian Unity Inova 500 MHz. The statistical data of particle sizes from SEM imaging and XRD analysis were obtained by Digimizer and High score plus software, respectively. DLS spectra were also obtained by a Horiba SZ-100 Nanoparticle Analyzer. Ultrasonic irradiation was performed in an ultrasound cleaning bath KQ-250 DE with a frequency of 50 kHz and power of 250 W L⁻¹.

3.2. Practical section

3.2.1. Preparation of iron oxide NPs

In a round-bottom flask (250 mL), a mixture of FeCl₃•6H₂O (10 mmol), FeCl₂•4H₂O (10 mmol) and deionized water (100 mL) were stirred and heated to about 60 °C. The stirring was continued for 30 min until the iron salts were dissolved in the water. Then, temperature was reached to 85 °C under N₂ atmosphere with rapid stirring for additional 2 h. A solution of concentrated aqueous ammonia (15 mL, 25 wt %) was added drop-wise to the solution for 1 h. Then the reaction mixture was cooled to room temperature and the resulting magnetic iron oxide NPs collected with an external magnet. Dark magnetic NPs were washed with water and ethanol several times. Finally, drying was done at 60 °C.

3.2.2. Preparation of silica-coated iron oxide NPs

The prepared iron oxide NPs (1.0 g) were initially dispersed in water (10 mL), ethanol (5 mL), PEG-300 (5 mL) and concentrated aqueous ammonia (1 mL, 28 wt %), by using an ultrasonic bath. Then, a solution of TEOS (2 mL) in ethanol (10 mL) was loaded drop by drop to the dispersion under stirring

was collected by magnetic separation and washed with ethanol. The light brown silica-coated iron oxide NPs were dried at 60 °C.

3.2.3. Preparation of the vinyl modified silica-coated iron oxide NPs

Initially, in a three-necked flask (100 mL) containing dry chloroform (70 mL), as-prepared silica-coated iron oxide NPs (10 g), that were prepared according to the literature, was charged. Then TMVS (3.54 g, 0.02 mol) was added to the reaction mixture drop-wise at room temperature. After completion of addition, the mixture was stirred for 12 h at the refluxing temperature of chloroform. Ultimately, the vinyl modified silica-coated iron oxide NPs were collected by using an external magnet and also washed with ethanol several times. Relatively rough particles were dried at 60 °C.

3.2.4. Preparation of Fe_3O_4/SiO_2 -PDA nanocatalyst

Firstly, vinyl modified Fe_3O_4/SiO_2 NPs (0.1 g) were well dispersed in deionized water (4.0 mL) via ultrasonication for 15 min. Next, an aqueous solution of melamine (50 ppm) was added drop by drop into the flask during the ultrasonication. Then, the mixture was put into the ultrasound bath (50 KHz) at 50 °C. After completion the reaction, magnetic NPs were simply collected from the reaction mixture by using an external magnet, washed with ethanol and then dried at 60 °C.

3.2.5. General procedure for co-catalyzed synthesis of 1,4-DHP derivatives (**5a–r**, **6a–e**) by Fe_3O_4/SiO_2 -PDA NPs and USW

Of each component, aldehyde **1** (1.0 mmol), ammonium acetate **2** (1.0 mmol), and β -keto ester **3** or dimedone **4** (2.0 mmol), in deionized water (2.0 mL) and in the presence of the fabricated Fe_3O_4/SiO_2 -PDA NPs (50 mg) were ultrasonicated (50 KHz) for 10 min, at room temperature. After completion of the reaction, the NPs were magnetically separated, and the residual product was collected by filtration and washed with ethanol and recrystallized to yield the pure product.

3.3. Spectral data of the selected products

ν/cm^{-1}): 3357, 1695, 1652, 1487, 1371, 1213; ^1H NMR (500 MHz, DMSO): δ_{H} (ppm) = 1.18 (s, 6H, CH_3), 2.32 (s, 6H, CH_3), 4.04 (m, 4H, CH_2 , broad), 4.90 (s, 1H, CH), 7.22-7.32 (m, 4H, H-Ar), 8.92 (s, 1H, NH); ^{13}C NMR (125 MHz, DMSO): δ_{C} (ppm) = 14.1, 18.2, 38.5, 59.0, 101.5, 127.8, 129.2, 130.4, 145.6, 147.1, 166.8.

Diethyl 2,6-dimethyl-4-(3-nitrophenyl)-1,4-dihydropyridine-3,5-dicarboxylate (5c): FT-IR (KBr: ν/cm^{-1}): 3346, 2987, 1704, 1647, 1487, 1348, 1213, 1118; ^1H NMR (500 MHz, DMSO): δ_{H} (ppm) = 1.20 (t, 6H, $J = 7.1$ Hz, CH_3), 2.33 (s, 6H, CH_3), 4.01-4.11 (m, 4H, CH_2), 4.90 (s, 1H, CH), 7.17 (d, 2H, $J = 8.4$ Hz, H-Ar), 7.47 (d, 2H, $J = 8.4$ Hz, H-Ar), 8.94 (s, 1H, NH).

Diethyl 2,6-dimethyl-4-(4-methoxyphenyl)-1,4-dihydropyridine-3,5-dicarboxylate (5f): FT-IR (KBr: ν/cm^{-1}): 3340, 2974, 1689, 1650, 1496, 1209, 1026, 838, 682; ^1H NMR (500 MHz, CDCl_3): δ_{H} (ppm) = 1.33 (t, 6H, $J = 7.1$ Hz, CH_3), 2.41 (s, 6H, CH_3), 3.86 (s, 3H, OCH_3), 4.20 (m, 4H, CH_2), 5.04 (s, 1H, CH), 6.01 (s, 1H, NH), 6.86 (d, 2H, $J = 8.5$ Hz, H-Ar), 7.31 (d, 2H, $J = 8.5$ Hz, H-Ar).

Diethyl 4-(4-bromophenyl)-2,6-dimethyl-1,4-dihydropyridine-3,5-dicarboxylate (5g): FT-IR (KBr: ν/cm^{-1}): 3357, 2989, 1693, 1652, 1488, 1377, 1217, 1012, 780; ^1H NMR (500 MHz, DMSO): δ_{H} (ppm) = 1.18 (s, 6H, CH_3), 2.32 (m, 6H, CH_3 , broad), 4.16-4.24 (m, 4H, CH_2 , broad), 4.90 (s, 1H, CH), 7.22-7.32 (m, 4H, H-Ar), 8.92 (s, 1H, NH); ^{13}C NMR (125 MHz, DMSO): δ_{C} (ppm) = 14.1, 18.2, 38.5, 59.0, 101.5, 127.8, 129.2, 130.4, 145.6, 147.1, 166.8.

Diethyl 2,6-dimethyl-4-(thiophen-2-yl)-1,4-dihydropyridine-3,5-dicarboxylate (5n): FT-IR (KBr: ν/cm^{-1}): 3344, 2985, 1695, 1652, 1487, 1371, 1299, 1209, 1124, 719; ^1H NMR (500 MHz, CDCl_3): δ_{H} (ppm) = 1.38 (t, 6H, $J = 7.1$ Hz, CH_3), 2.45 (s, 6H, CH_3), 4.25-4.32 (m, 4H, CH_2), 5.46 (s, 1H, CH), 5.97 (s, 1H, NH), 6.90-6.97 (m, 2H), 7.47 (dd, 1H, $J = 1.2$ Hz, $J = 3.9$ Hz, H-Ar).

Herein, preparation of pyrimidine-2,4-diamine-functionalized silica-coated magnetic nanoparticles ($\text{Fe}_3\text{O}_4/\text{SiO}_2\text{-PDA}$ NPs) as an efficient co-catalyst for synthesis of 1,4-dihydropyridine (1,4-DHP) derivatives via three different methods has been presented. According to the obtained results, among reflux, MW and USW irradiations techniques, well-functionalized (through covalent bonding) monodispersed particles have been fabricated via ultrasonication (in the ultrasonic bath with power density 250 W L^{-1} and frequency 50 kHz) in comparison with two other methods. In this study, it has been proven that the core/shell structure of the magnetic NPs is greatly preserved from damaging and the particle accumulation (as a negative event) is well inhibited by ultrasonication. Additionally, it has been shown that the physical adsorption is occurred via MW irradiation method. These claims have been proven by various analysis methods such as FT-IR, EDX, TEM, SEM, DLS and XRD, after several times washing the NPs. Furthermore, the obtained high reaction yields (89%) for synthesis of 1,4-DHP derivatives (as important pharmaceutical compounds) via efficient co-catalyzing by the prepared $\text{Fe}_3\text{O}_4/\text{SiO}_2\text{-PDA}$ NPs and USW irradiation, have disclosed this fact that a substantial catalytic activity is executed through a synergistic effect between PDA-functionalized magnetic NPs and USWs.

Abbreviations

NPs = Nanoparticles

PDA = pyrimidine-2,4-diamine

1,4-DHP = 1,4-dihydropyridine

USW = Ultrasound wave

MW = microwave

TEOS = Tetraethyl orthosilicate

TMVS = Trimethoxy vinylsilane

The authors gratefully acknowledge the partial support from the Research Council of the Iran University of Science and Technology and the Iran National Science Foundation (INSF).

Conflict of Interest

The authors declare no conflict of interest.

Supporting Information

The SI file includes FT-IR spectra and original $^1\text{H-NMR}$ and $^{13}\text{C-NMR}$ spectra of selected 1,4-dihydropyridine products.

References

- [1] E. Ruiz, H. Rodríguez, J. Coro, V. Niebla, A. Rodríguez, R. Martínez-Alvarez, H.N.D. Armas, M. Suárez, N. Martín, Efficient sonochemical synthesis of alkyl 4-aryl-6-chloro-5-formyl-2-methyl-1,4-dihydropyridine-3-carboxylate derivatives, *Ultrason. Sonochem.* 19 (2012) 221-226.
- [2] H. Haller, Effective management of hypertension with dihydropyridine calcium channel blocker-based combination therapy in patients at high cardiovascular risk, *Int. J. Clin. Pract.* 65 (2008) 781-790.
- [3] Y.B. Xie, S.P. Ye, W.F. Chen, Y.L. Hu, D.J. Li, L. Wang, Brønsted- acid- catalyzed multicomponent one- Pot reaction: efficient synthesis of polysubstituted 1,2- dihydropyridines, *Asian J. Org. Chem.* 6 (2017) 746-750.
- [4] L. Jiang, W. Ye, W. Su, One-pot multicomponent synthesis of highly functionalized 1,4-dihydropyridines using porcine pancreatic lipase, *Chem. Res. Chinese. U.* 35 (2019) 235-238.
- [5] A. Maleki, R. Firouzi-Haji, Z. Hajizadeh, Magnetic guanidinylated chitosan nanobiocomposite: a green catalyst for the synthesis of 1,4-dihydropyridines, *Int. J. Biol. Macromol.* 116 (2018) 320-326.

- synthesis of functionalized 1-(2-fluorophenyl)-1,4-dihydropyridines under ultrasound irradiation, *New J. Chem.* 40 (2016) 5107-5112.
- [7] S. Tabassum, S. Govindaraju, R.R. Khan, M. A. Pasha, Ultrasound mediated, green innovation for the synthesis of polysubstituted 1,4-dihydropyridines, *RSC Adv.* 6 (2016) 29802-29810.
- [8] D. Wang, W. Luo, G. Wen, L. Yang, S. Hong, S. Zhang, J. Diao, J. Wang, H. Wei, Y. Li, Y. Wang, Synergistic effects of negative-charged nanoparticles assisted by ultrasound on the reversal multidrug resistance phenotype in breast cancer cells, *Ultrason. Sonochem.* 34 (2017) 448-457.
- [9] S.G. Babu, P. Karthik, M.C. John, S.K. Lakhera, M. Ashokkumar, J. Khim, B. Neppolian, Synergistic effect of sono-photocatalytic process for the degradation of organic pollutants using CuO-TiO₂/rGO, *Ultrason. Sonochem.* 50 (2019) 218-223.
- [10] P. Bansal, G. R. Chaudhary, S. K. Mehta, Comparative study of catalytic activity of ZrO₂ nanoparticles for sonocatalytic and photocatalytic degradation of cationic and anionic dyes, *Chem. Eng. J.* 280 (2015) 475-485.
- [11] M. Yang, K. Du, Y. Hou, S. Xie, Y. Dong, D. Li, Y. Du, Synergistic antifungal effect of amphotericin B-loaded poly(lactic-co-glycolic acid) nanoparticles and ultrasound against candida albicans biofilms, *Antimicrob. Agents Chemother.* 63 (2019) 2022-2040.
- [12] S. Sumitomo, H. Koizumi, Md.A. Uddin, Y. Kato, Comparison of dispersion behavior of agglomerated particles in liquid between ultrasonic irradiation and mechanical stirring, *Ultrason. Sonochem.* 40 (2018) 822-831.
- [13] A. Maleki, R. Taheri- Ledari, M. Soroushnejad, Surface functionalization of magnetic nanoparticles via palladium- catalyzed Diels- Alder approach, *ChemistrySelect*, 3 (2018) 13057-13062.
- [14] G. Bhanjana, P. Rana, G. R. Chaudhary, N. Dilbaghi, K. H. Kim & S. Kumar, Manganese oxide nanochips as a novel electrocatalyst for direct redox sensing of hexavalent chromium, *Sci. Rep.* 9 (2019) 2045-2322.

dyes from water with the synergistic effect of Ni doped ZnO nanoparticles and ultrasonication, *Ultrason. Sonochem.* 22 (2015) 317-325.

[16] A. Maleki, R. Taheri-Ledari, J. Rahimi, M. Soroushnejad, Z. Hajizadeh, Facile peptide bond formation: Effective interplay between isothiazolone rings and silanol groups at silver/iron oxide nanocomposite surfaces, *ACS Omega*, 4 (2019) 10629-10639.

[17] A. Maleki, M. Niksefat, J. Rahimi, R. Taheri-Ledari, Multicomponent synthesis of pyrano[2,3-d]pyrimidine derivatives via a direct one-pot strategy executed by novel designed copperated Fe_3O_4 @polyvinyl alcohol magnetic nanoparticles, *Mater. Today Chem.* 13 (2019) 110-120.

[18] Y. Areerob, J.Y. Cho, W.K. Jang, W.C. Oh, Enhanced sonocatalytic degradation of organic dyes from aqueous solutions by novel synthesis of mesoporous Fe_3O_4 -graphene/ZnO@SiO₂ nanocomposites, *Ultrason. Sonochem.* 41 (2018) 267-278.

[19] S. Mallakpour, H.Y. Nazari, Ultrasonic-assisted fabrication and characterization of PVC-SiO₂ nanocomposites having bovine serum albumin as a bio coupling agent, *Ultrason. Sonochem.* 39 (2017) 686-697.

[20] Y. Snoussi, S. Bastide, M. Abderrabba, M.M. Chehimi, Sonochemical synthesis of Fe_3O_4 @NH₂-mesoporous silica@Polypyrrole/Pd: A core/double shell nanocomposite for catalytic applications, *Ultrason. Sonochem.* 41 (2018) 551-561.

[21] S. Bhattacharjee, DLS and zeta potential – What they are and what they are not?, *J. Control. Release*, 235 (2016) 337–351.

[22] S. Mallakpour, M. Javadpour, Sonochemical assisted synthesis and characterization of magnetic PET/Fe₃O₄, CA, AS nanocomposites: Morphology and physiochemical properties, *Ultrason. Sonochem.* 40 (2018) 611-618.

[23] A. Heydari, S. Khaksar, M. Tajbakhsh, H.R. Bijanzadeh, One-step, synthesis of Hantzsch esters and polyhydroquinoline derivatives in fluoro alcohols, *J. Fluorine Chem.* 130 (2009) 609-614.

Aromatization of Hantzsch 1,4-dihydropyridines with manganese dioxide and 2,3-dichloro-5,6-dicyano-1,4-benzoquinone, *Tetrahedron* 51 (1995) 6511-6516.

[25] D.S. Rekunge, C.K. Khatri, G.U. Chaturbhuj, Sulfated polyborate: An efficient and reusable catalyst for one pot synthesis of Hantzsch 1,4-dihydropyridines derivatives using ammonium carbonate under solvent free conditions, *Tetrahedron Lett.* 58 (2017) 1240-1244.

[26] B. Jahanbin, A. Davoodnia, H. Behmadi, N. Tavakoli-Hoseini, Polymer support immobilized acidic ionic liquid: Preparation and its application as catalyst in the synthesis of hantzsch 1,4-dihydropyridines, *Bull. Korean Chem. Soc.* 33 (2012) 2140-2144.

[27] R.F. Affeldt, R.S. Iglesias, F.S. Rodembusch, D. Russowsky, Photophysical properties of a series of 4- aryl substituted 1,4- dihydropyridines, *J. Phys. Org. Chem.* 25 (2012) 769-777.

[28] N. Taheri, F. Heidarizadeh, A. Kiasat, A new magnetically recoverable catalyst promoting the synthesis of 1,4-dihydropyridine and polyhydroquinoline derivatives via the Hantzsch condensation under solvent-free conditions, *J. Magn. Magn. Mater.* 428 (2017) 481-487.

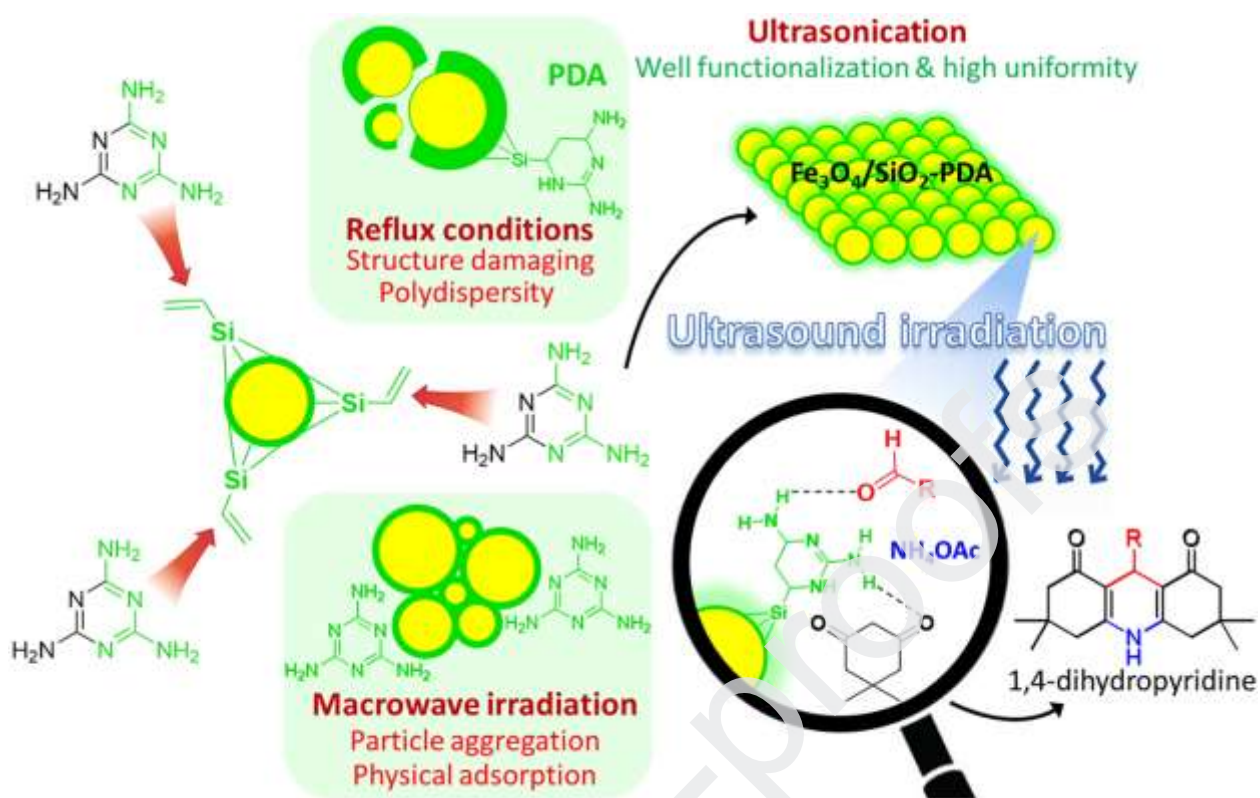
[29] T.D. Ananda Kumar, P. Mohan, C. Subrahmanyam, K. Satyanarayana, Comparative Study of Catalytic Potential of TBAB, BTEAC, and CTAB in One-Pot Synthesis of 1,4-Dihydropyridines Under Aqueous Medium, *Synth. Commun.* 44 (2014) 574-582.

[30] B.M. Khadilkar, V.G. Gaikar, A.A. Chitnavis, Aqueous hydrotrope solution as a safer medium for microwave enhanced hantzsch dihydropyridine ester synthesis, *Tetrahedron Lett.* 36 (1995) 8083-8086.

[31] H.R. Memarian, M. Bagheri, D. Döpp, Synthesis and photochemistry of novel 3, 5-diacetyl-1, 4-dihydropyridines, *Monatsh. Chem.* 135 (2004) 833-838.

[32] B. Mu, W. Wang, J. Zhang, A. Wang, Superparamagnetic sandwich structured silver/halloysite nanotube/Fe₃O₄ nanocomposites for 4-nitrophenol reduction, *RSC Adv.* 4 (2014) 39439-39445.

[33] A.K. Dutta, P. Gogoi, R. Borah, Synthesis of dibenzoxanthene and acridine derivatives catalyzed by 1,3-disulfonic acid imidazolium carboxylate ionic liquids, *RSC Adv.* 4 (2014) 41287-41291.



Highlights

- Precise comparison between reflux, microwave and ultrasound irradiation methods
- Synergistic catalytic effect between magnetic nanoparticles and ultrasound waves
- Convenient preparation of $\text{Fe}_3\text{O}_4/\text{SiO}_2$ -PDA as an efficient nanocatalyst
- High reaction yields for co-catalyzed synthesis of 1,4-dihydropyridine derivatives
- Electronic resonance enhancement by ultrasound wave irradiation in nanocatalysis